

A Two-Dimensional Unsteady FDTD Model for Radon Transport with Multiple Sources Emanation from Soil Layers

H. Bezzout*, E. H. El Ouardy, N. Meskini, H. El Faylali

Department of Physics and Computer Science, Faculty of Sciences, Ibn Tofail University, University Campus Pbox 133, Kenitra, Morocco

ARTICLE INFO

Article history:

Received 23 March 2022

Received in revised form 18 January 2023

Accepted 24 January 2023

Keywords:

Radon transport
Diffusion coefficient
Convection velocity
FDTD method
Radon multi-sources
Porous media

ABSTRACT

A two-dimensional numerical model for radon transport based on the finite difference time domain (FDTD) method have been developed. The model is governed by the radon transport equation taking into account the mechanisms of diffusion, advection, and decay. The purpose of this model is to simulate the evolution of radon concentration which can be influenced by various parameters including depth and diffusion coefficient of the soil layer plus the velocity and initial concentration of radon. The obtained results were compared to an analytical solution to demonstrate the ability of this model for predicting the spatio-temporal evolution of radon transport in the porous media of soil layers.

© 2023 Atom Indonesia. All rights reserved

INTRODUCTION

Radon is an odorless and colorless radioactive gas that occurs naturally from soil and rocks. R_n^{222} is the most important isotope that can be transported from the depths of the ground to the surface without reacting with other types of atoms. Due to its density and radioactive properties, the radon gas in the ground can be used to detect rock types or evaluate the subsurface flows to predict the productivity of the ecological zoning [1]. Through this transport mechanism, radon produced in the ground is potentially hazardous to lung health when transported to the surface and inhaled by humans [2]. In several cases, the most dominant transport mechanism is the diffusion mechanism which is enabled by the variation of radon concentration in the ground and in the surface [2].

Different techniques are used for modeling the transport of radon in different types of materials. Some studies have investigated the transport of radon in buildings, especially in bricks. Due to the dominance of the radon diffusion mechanism, the concentration of radon in buildings is influenced by the diffusion coefficient and the permeability of

bricks [3]. Sabbarese et al. [4] used a one dimensional configuration for studying the concentration of radon in dwelling and the effect of materials properties with the position of lower floor on the indoor concentration of radon. Campos et al. [5] examined the measurement of radon exhalation rate in bricks made of phosphogypsum. A simulation based on the Monte-Carlo method allows to model the transport of radon from soil to air in one dimension at a steady state condition [6]. In addition, the modeling of uncertainties in soil parameters such as diffusivity and convection velocity provides an approximation to the real case of measurement with uncertainties. Thus, the variation of the radon activity concentration depends on the convection velocity [7].

The finite difference time domain (FDTD) [8-11] is a numerical method based on the discretization of time and space of the problem proposed. It is highly used in the electromagnetic domain and telecommunication to solve the Maxwell's equations with different types of boundary conditions [12-14]. Several algorithms were proposed for increasing the efficiency of this method, for example, the auxiliary differential equation (ADE) FDTD that is applied for dispersive structures [15] and magnetized plasma [16]. Some research studies have employed FDTD

*Corresponding author.

E-mail address: hamid.bezzout@gmail.com

DOI: <https://doi.org/10.55981/aij.2023.1230>

method for modeling patch antenna based on the three dimensional algorithm for FDTD [17] and dipole antenna [18].

In this paper, a new 2D-FDTD algorithm is proposed for radon transport in two dimensions based on the FDTD method. This model combines space and time variation of radon rate and simulates the effect of different parameters such as the convection velocity and the number of radon sources, and the radon concentration rate.

Furthermore, the simulated results obtained by this model are compared with solutions found in the previous works [19-20]. According to the one-source solution described in [21], the multi-source solution can be obtained using initial and boundary conditions of the configuration described in the following sections. To the best of our knowledge, there is no FDTD model adapted to the simulation of multi-source radon transport with convection mechanism. So, the results from our model have shown a good correlation.

METHODS AND MODELS

Geometric model

This work investigates the variation of the radon gas concentration in soil layers coming initially from a single source, with and without convection mechanism. Then, to simulate the case close to reality, multiple sources are also investigated.

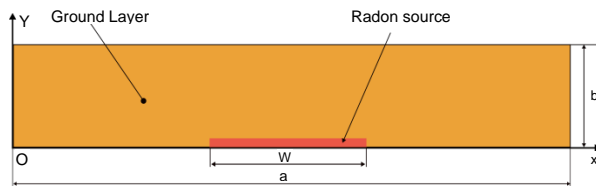


Fig. 1. A two-dimensional configuration of ground layer for a single source.

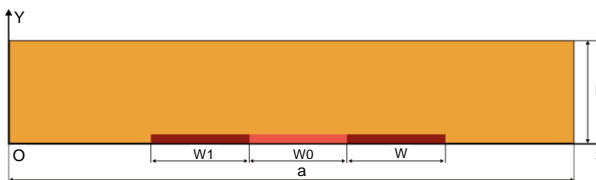


Fig. 2. A two-dimensional representation of ground layer and multiple sources.

In this paper, Python language was used to implement the model owing to its computational robustness and coding simplicity. A two-dimensional configurations with a dimension of $a \times b$ are shown in Fig. 1 and Fig. 2, where

$a = 26 \text{ m}$, $b = 2.8 \text{ m}$. For the single source, the width of the source is $w = 6 \text{ m}$, and for multiple sources, shown in Fig. 2, the dimension of sources is $W_0 = W_1 = W_2 = 4.5 \text{ m}$. Two scenarios of source concentration in multiple sources were simulated, e.g. scenario (a) three sources of radon are assumed in the same depth with the concentration of central source, W_0 was assumed as C_0 , and the two other sources assumed as $C_1 = C_2 = 2 C_0$, and scenario (b), three sources of radon were assumed in the same depth, with the concentrations were $C_1 = C_2 = 0.5 C_0$.

Governing equations

The evolution of the radon concentration from a source located at a certain depth in the ground depends on several factors, such as the width of the radon source, its depth in the ground, the composition of the ground layers and the transport velocity due to the convection mechanism. Fig. 1 describes the configuration of radon in two dimensions, where a and b are the dimensions of the ground layer, and w is the width of the source. In order to model the transport of radon in a porous media (ground layer) relative to the Fig. 1, the following transport equation is used in Eq. (1):

$$\frac{\partial C_{Rn}}{\partial t} = D_e \nabla^2 C_{Rn} - V \nabla C_{Rn} - \lambda C_{Rn} + Q \quad (1)$$

Equation (1) is composed of four components of transport mechanisms; diffusion, advection, decay and generation, where C_{Rn} is the concentration of radon per unit volume in $Bq \text{ m}^{-3}$, D_e is the diffusion coefficient in $\text{m}^2 \text{ s}^{-2}$, λ is the decay constant of R_n^{222} ($2.07 \cdot 10^{-6} \text{ s}^{-1}$), V is the velocity of Darcy due to the advection mechanism in $\text{m} \cdot \text{s}^{-1}$, Q is the generation number of atoms due to the generation mechanism in $(\text{m}^3 \cdot \text{s}^{-1})$.

In this study, two dimensional radon transport hypothesis was considered, assuming that radon gas is transported from the source to the air-soil interface with Eq. (2).

$$\nabla^2 C_{Rn} = \left(\frac{\partial C_{Rn}}{\partial x} \right)^2 + \left(\frac{\partial C_{Rn}}{\partial y} \right)^2 \quad (2)$$

By substituting Eq. 2 to Eq. 1, the transport equation in two dimension is described in Eq. (3)

$$\frac{\partial C_{Rn}}{\partial t} = D_e \times \left(\left(\frac{\partial C_{Rn}}{\partial x} \right)^2 + \left(\frac{\partial C_{Rn}}{\partial y} \right)^2 \right) - V \times \left(\frac{\partial C_{Rn}}{\partial y} \right) - \lambda C_{Rn} + Q \quad (3)$$

By applying the central finite difference scheme in time and space (FDTD) to partial derivatives of time and space in Eq. (3), then Eq. (4) is obtained as follows.

$$C_{Rn}|_{i,j}^{n+1} = A \times C_{Rn}|_{i,j}^n + B \times C_{Rn}|_{i+1,j}^n + C \times C_{Rn}|_{i-1,j}^n + D \times (C_{Rn}|_{i,j+1}^n - C_{Rn}|_{i,j-1}^n)$$

where:

$$A = 1 - De \frac{\Delta t.(\Delta x^2 + \Delta y^2)}{\Delta x^2.\Delta y^2} - V \frac{\Delta t}{\Delta x} - \lambda \Delta t$$

$$B = De \frac{\Delta t}{\Delta x^2}, C = \frac{\Delta t.(V.\Delta x - De)}{\Delta x^2}, D = De \frac{\Delta t}{\Delta y^2}$$

Boundary conditions

To define our numerical model in space and time, the initial and boundary conditions expressed in Eq. (5) were applied for a single source of radon shown in Fig. 1.

$$\begin{cases} C_{Rn}(x, y) = 0, \text{ if } \begin{cases} x = 0 \\ x = a \end{cases} \\ C_{Rn}(x, 0) = C_0, \text{ if } \begin{cases} x < \frac{(a+w)}{2} \\ x > \frac{(a-w)}{2} \end{cases} \end{cases} \quad (5)$$

For multiple sources emanation depicted in Fig. 2, the initial and boundary conditions expressed in Eq. (6) and Eq. (7) were applied.

$$\begin{cases} C_{Rn}(x, y) = 0, \text{ if } \begin{cases} x = 0 \\ x = a \end{cases} \\ C_{Rn}(x, 0) = C_0, \text{ if } \begin{cases} x < \frac{(a+w_0)}{2} \\ x > \frac{(a-w_0)}{2} \end{cases} \end{cases} \quad (6)$$

$$\begin{cases} C_{Rn}(x, y) = C_2, \text{ if } \begin{cases} x < \frac{(a+w_0)}{2} + w_2 \\ x > \frac{(a-w_0)}{2} \end{cases} \\ C_{Rn}(x, 0) = C_1, \text{ if } \begin{cases} x = \frac{(a-w_0)}{2} \\ x = \frac{(a-w_0)}{2} - w_1 \end{cases} \end{cases} \quad (7)$$

Implementation of the program

To implement numerically the equation of radon transport defined by Eq. (3), the FDTD method is needed to discretize space and time evolution which gives the Eq. (4). By adding the boundary conditions, Eqs. 5-7 were also added to the FDTD model. The final algorithm

which is called (RadonTransport-FDTD) is presented in Fig. 3.

Algorithm 1: RadonTransport-FDTD

```

1 Initialize  $n_x, n_y, nt$ 
2 Initialize Boundary conditions using equations (5) and (6)
3 Calculate Update coefficients, A, B, C, and D
4 while  $n < n_t$  do
5   while  $j < n_y$  do
6     while  $i < n_x$  do
7       Update  $C_{Rn,j,i}^n$  using equation (4)
8     end
9   end
10 end
    
```

Fig. 3. Radon FDTD algorithm based on central finite difference scheme.

RESULTS AND DISCUSSION

Influence of the convection velocity on the radon concentration rate with single source

A study of radon transport in terrestrial layers using the FDTD method has been conducted by A. Tayebi et al. [17], with only one radon source and having no convection mechanism. In this work, the convection mechanism is included in the model by adding the convection velocity parameter. The computation of radon concentration at different depths based on this FDTD-radon transport model, in the case without convection (Fig. 4(a)) and with convection (Fig. 4(b)) shows that the existence of convection increases the emanation rate, hence the probability of detecting the source at soil surface also increases.

By comparing the results obtained with the analytical solution in different depths ($Y = 2.1 \text{ m}$), ($Y = 1.4 \text{ m}$), ($Y = 0 \text{ m}$) as shown in Fig. 4(c), these two methods show a good agreement. Both methods show that the emanation rate is maximum over the source and over its whole width.

In this work, multiples sources with different dimensions were modeled. In the Scenario 1, the central source assumed as C_0 and the two other sources assumed as C_1 and C_2 with $C_1 = C_2 = 2 C_0$. Figure 5 shows the concentration rate of radon in two dimensions at different iteration (n) steps, respectively at $n = 11$ (Fig. 5(a)), $n = 91$ (Fig. 5(b)), $n = 301$ (Fig. 5(c)), and $n = 500$ (Fig. 5(d)), in the last iteration ($n = 500$), the radon has reached the soil surface with low concentration, and dependent to the form of sources generated in the soil layers.

2

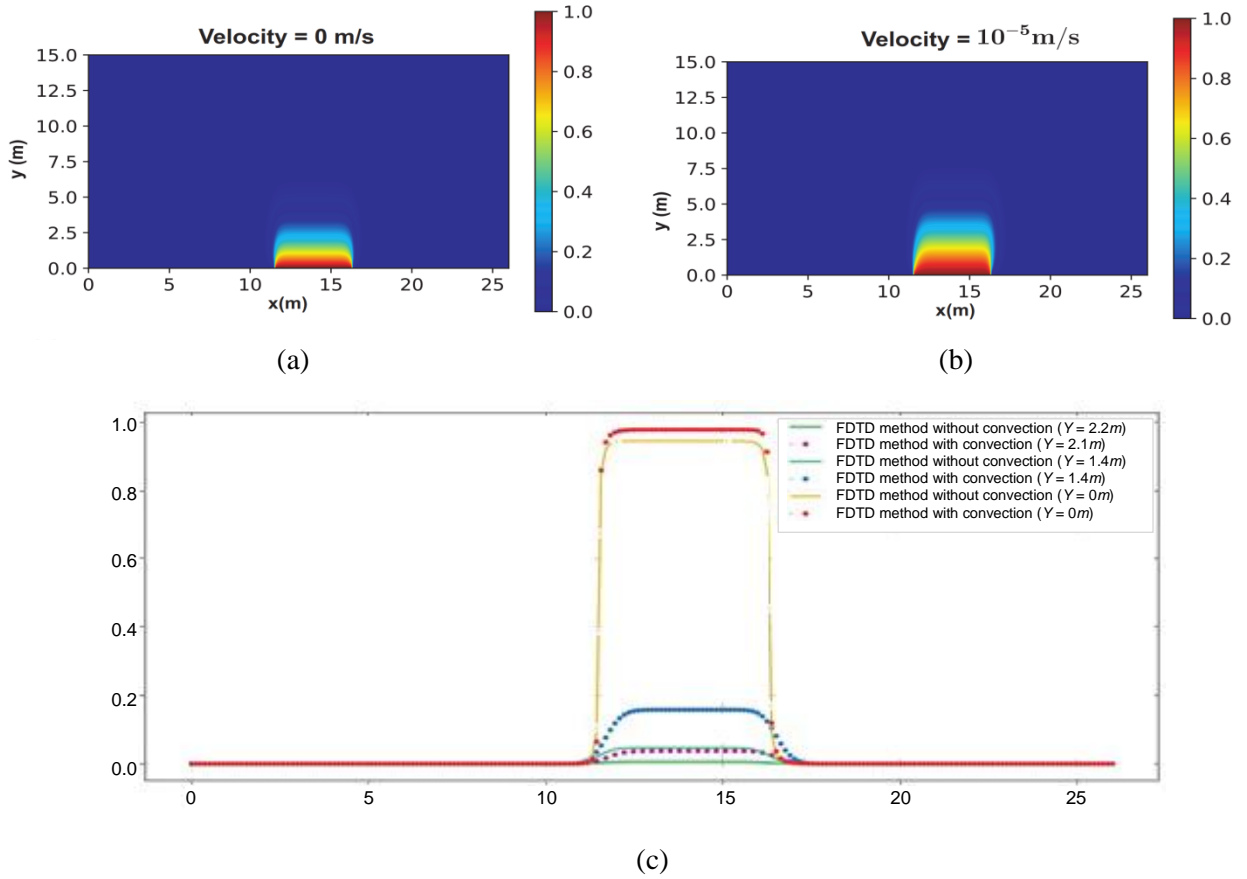


Fig. 4. Radon concentration rate based on simulation by taking into account the effect of convection velocity using FDTD and based on analytic solution.

3

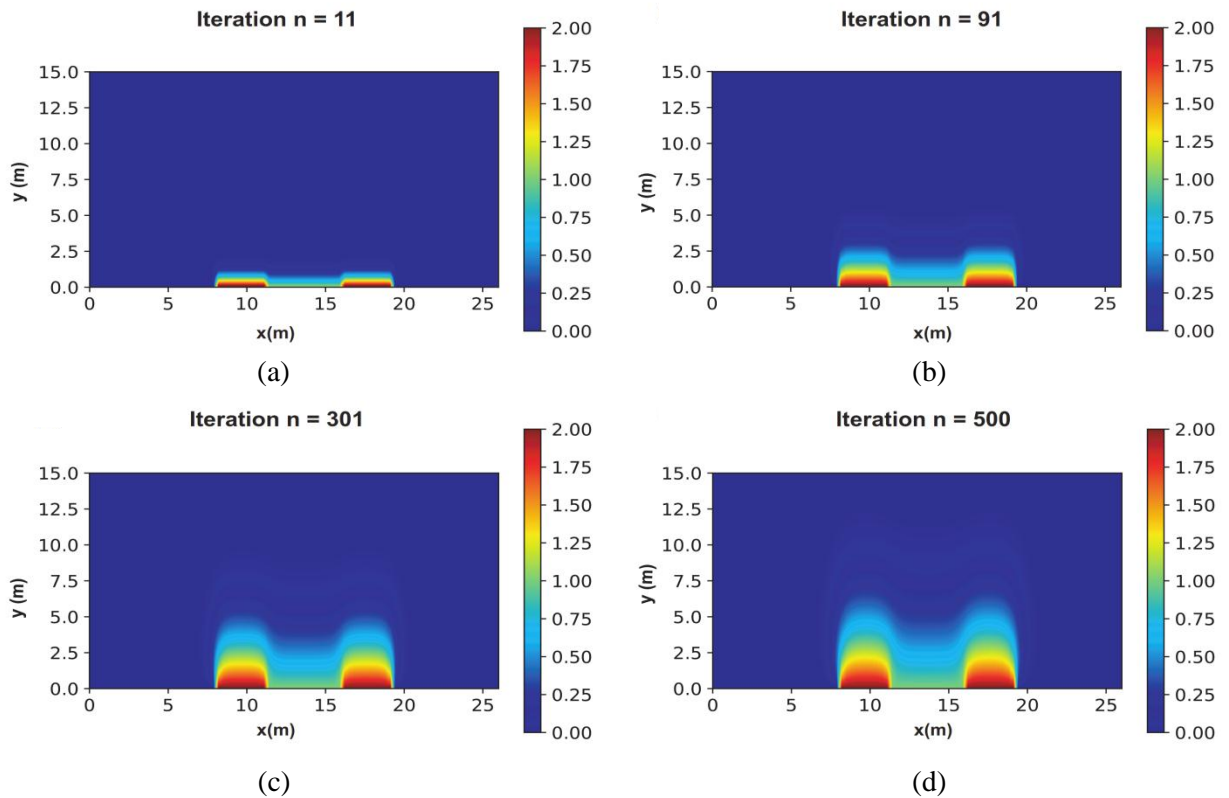
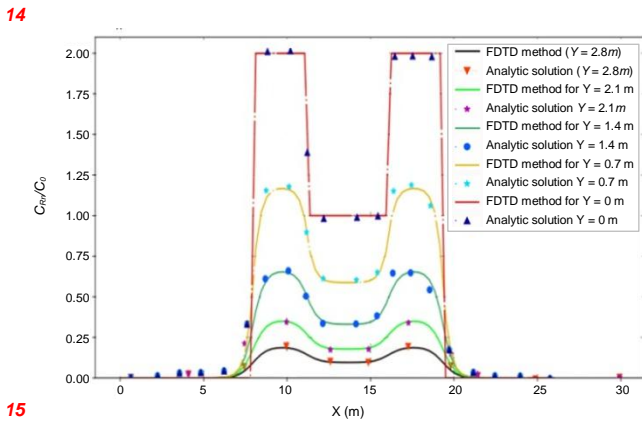


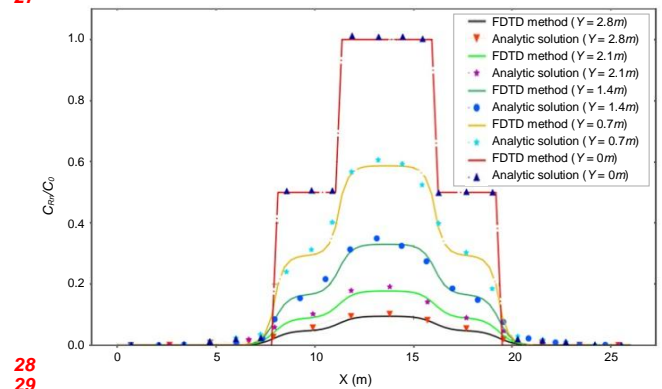
Fig. 5. Scenario 1: Two-dimensional FDTD solution with different time steps.

4
 5 Figure 6 shows the radon concentration rate
 6 (C_{Rn}/C_0) that evolves through the depth (Y). For
 7 ($Y = 0$), which is equivalent to 2.8 m in depth, the
 8 radon concentration is maximum ($\frac{C_{Rn}}{C_0} = 2$), while
 9 the radon transports through ground layers and
 10 reach ground surface ($Y = 2.8 m$) with a
 11 concentration rate of ($\frac{C_{Rn}}{C_0} = 0.125$). The results of
 12 this model are in a good agreement with the results
 13 of analytical solution.

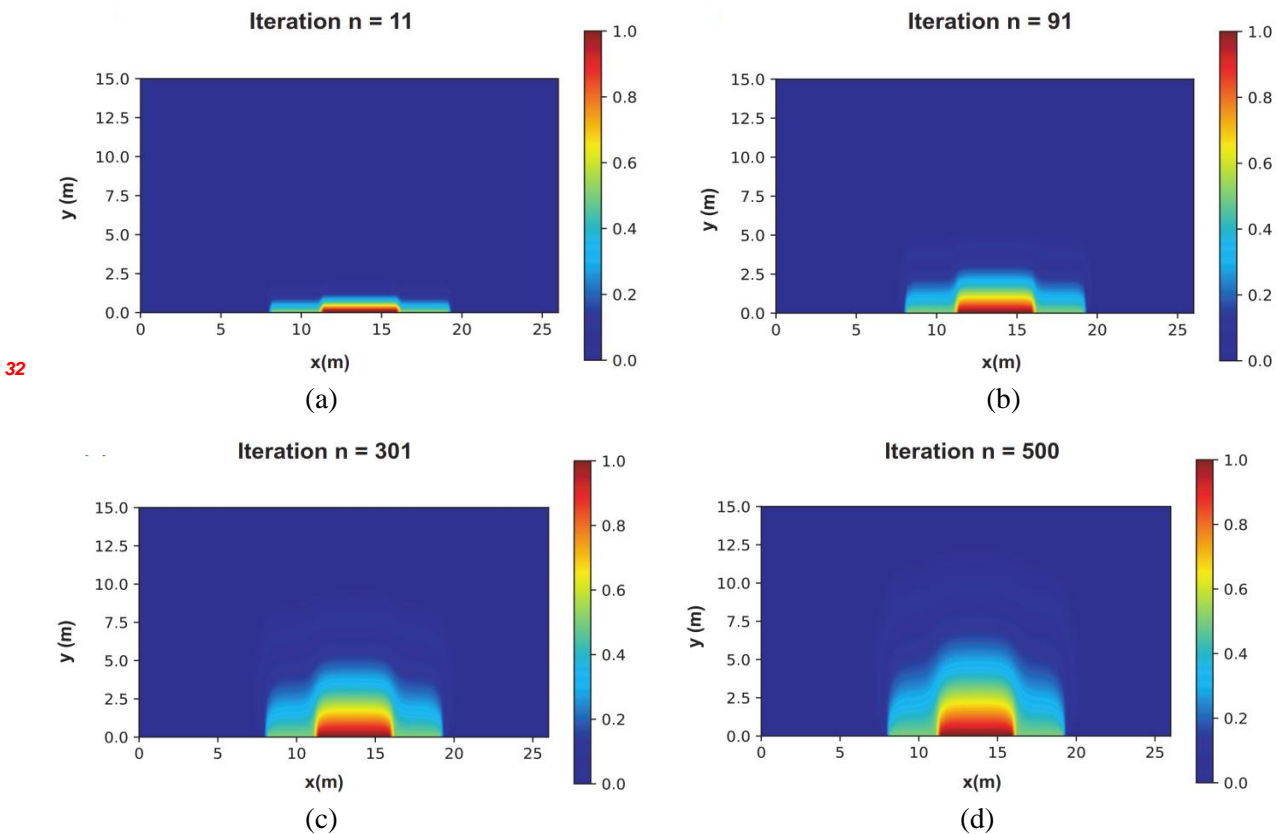


14
 15
 16
 17
 18
 19
 20
 21
 22
 23
 24
 25
 26
 27
 28
 29
 30
 31
Fig. 6. Scenario 1: evolution of radon concentration rate of multiple sources at differents depths.

16 In scenario 2, a configuration has been made
 17 with initial radon sources as $C_1 = C_2 = 0.5C_0$.
 18 Fig. 7 shows the evolution of radon concentration rate
 19 in two dimensions through time. In addition,
 20 this scenario is characterized by a high concentration
 21 in the central source. It shows that the emanation
 22 rate in central source reach the soil surface in the
 23 first followed by the particles of radon in the adjacent
 24 sources. Figure 8 shows the radon concentration
 25 rate in different depths compared with the analytical
 26 solution. Both results show a good agreement.



28
 29
 30
 31
Fig. 7. Scenario 2: evolution of radon concentration rate of multiple sources at different depths.



32
 33
 34
 35
 36
 37
 38
 39
 40
 41
 42
 43
 44
 45
 46
 47
 48
 49
 50
 51
 52
 53
 54
 55
 56
 57
 58
 59
 60
 61
 62
 63
 64
 65
 66
 67
 68
 69
 70
 71
 72
 73
 74
 75
 76
 77
 78
 79
 80
 81
 82
 83
 84
 85
 86
 87
 88
 89
 90
 91
 92
 93
 94
 95
 96
 97
 98
 99
 100
Fig. 8. Scenario 2: Two dimensional FDTD solution with different time steps.

From the results obtained by the FDTD model, it is clarified that the process of radon transport in soil layers can be simulated by taking into account the influence of the convection velocity for multiple radon sources. These findings allow us to measure the dimension of sources. As shown in Fig. 8, the width at 75 % of the concentration rate is the width of the central source ($W = 4.5 \text{ m}$) named (W_0), and the width at 25 % of concentration rate is the width of the three sources. Therefore, the width of the two sources can be determined as $W_0 + W_1 + W_2 = W_{25\%}$ in scenario 1 and $W_1 = W_2$, so $W_1 = \left(\frac{W_{25\%} - W_0}{2}\right)$ in scenario 2, which give $W_1 = W_2 = 4.5 \text{ m}$ as mentioned in the previous configurations. As discussed by Yakovleva et al. [22], the radon activity concentration depends on the convection velocity and the characteristics of soil layers.

51

52

53 CONCLUSION

The simulation results based on the developed transport model reveal that the concentration rate of radon increase with convection velocity, which means that the concentration at the soil surface will be increased. This allows the detection of radon by sensors in the soil surface. For multiple sources of radon, the evolution of the concentration rate depends on the depth of the source which decreases by reaching the soil surface. The obtained results permit us to determine the width of the radon sources. The calculation results of the proposed FDTD model are in a good agreement with the analytical solution. So, the proposed model is reliable for simulation of the radon transport phenomenon in two dimensional space-time configuration with multiples sources.

71

72

73 AUTHOR CONTRIBUTION

Hamid Bezzout is the main contributor to this paper. He developed the input file, conducted the calculations, and wrote the manuscript. All other authors read and approved the final version of the paper.

79

80

81 REFERENCES

1. M. Sadat-Noori, C. Anibas, M. S. Andersen et al., *J. Hydrol.* **598** (2021) 126281.

125

126

2. J.-K. Kang, S. Seo and Y. W. Jin, *Yonsei Med. J.* **60** (2019) 597.
3. S. R. Soniya, S. Abraham, M. U. Khandaker et al., *Radiat. Phys. Chem.* **178** (2021) 108955.
4. C. Sabbarese, F. Ambrosino and A. D'Onofrio, *J. Environ. Radioact.* **227** (2021) 106501.
5. M. P. Campos, L. J. P. Costa, M. B. Nisti et al., *J. Environ. Radioact.* **172** (2017) 232.
6. A. Muhammad and F. K ulahcı, *J. Atmos. Sol. Terr. Phys.* **227** (2022) 105803.
7. S. Chakraverty, B. K. Sahoo, T. D. Rao et al., *J. Environ. Radioact.* **182** (2018) 165.
8. Q. Lei, J. Wang, J. L. Wang et al., *Antennas Wirel. Propag. Lett.* **16** (2017) 2824.
9. B. Yao, Q. Zheng, J. Peng et al., *Antennas Wirel. Propag. Lett.* **10** (2011) 866.
10. J.-P. Berenger, *IEEE Trans. Electromagn. Comput.* **47** (2005) 1008.
11. F. Bert -Rosell , E. Xifr -P rez, J. Ferr -Borrull et al., *Results Phys.* **11** (2018) 1008.
12. J. Zhou and J. Zhao, *IEEE Microwave Wireless Compon. Lett.* **22** (2012) 167.
13. J. A. Pereda, A. Serroukh, A. Grande et al., *Antennas Wirel. Propag. Lett.* **11** (2012) 981.
14. T. Ohtani, Y. Kanai and J. B. Cole, *IEEE Trans. Magn.* **49** (2013) 1569.
15. M. A. Alsunaidi and A. A. Al-Jabr, *IEEE Photonics Technol. Lett.* **21** (2009) 817.
16. B. T. Nguyen, A. Samimi, S. E. W. Vergara et al., *IEEE Trans. Antennas Propag.* **67** (2018) 438.
17. A. A. Sofi, S. Amit and B. K. Sujatha, *Global Transitions Proc.* **2** (2021) 323.
18. B. Shahmohamadi, R. S. Shirazi, G. Moradi et al., *Int. J. Electron. Commun.* **145** (2022) 154066.
19. V. Batu, *Water Resour. Res.* **29** (1993) 2881.
20. J. Simunek and D. L. Suarez, *Water Resour. Res.* **30** (1994) 1115.
21. A. Tayebi, H. Bezzout, M. El Maghraoui et al., *Atom Indones.* **46** (2020) 171.
22. V. S. Yakovleva and R. I. Parovik, *Nukleonika* **55** (2010) 601.